Korean Journal of Remote Sensing, Vol.21, No.5, 2005, pp.417~423

MRF-based Fuzzy Classification Using EM Algorithm

Sanghoon Lee †

Kyungwon University

Abstract : A fuzzy approach using an EM algorithm for image classification is presented. In this study, a double compound stochastic image process is assumed to combine a discrete-valued field for region-class processes and a continuous random field for observed intensity processes. The Markov random field is employed to characterize the geophysical connectedness of a digital image structure. The fuzzy classification is an EM iterative approach based on mixture probability distribution. Under the assumption of the double compound process, given an initial class map, this approach iteratively computes the fuzzy membership vectors in the E-step and the estimates of class-related parameters in the M-step. In the experiments with remotely sensed data, the MRF-based method yielded a spatially smooth class-map with more distinctive configuration of the classes than the non-MRF approach.

Key Words : Image classification, fuzzy method, Markov random field, EM algorithm.

1. Introduction

One of the most problems in image processing involves allocating the pixels in a given image to a number of classes according to their statistical properties. In statistical image classification, Markov random field (MRF) models (Kindermann and Snell, 1982) have been used for over a decade to characterize geophysical connectedness. The MRF represents the local characteristics of image structure such that neighboring pixels have a higher probability of being of the same class. Image classification based on an MRF has been used extensively for analysis of textured images in computer vision (Bouman and Liu, 1991; Manjunath and Chellappa, 1991; Won and Derin, 1992; Nguyen and Cohen, 1993; Kervrann and Heitz, 1995; Panjwani and Healey, 1995; Andrey and Tarroux, 1998). In this approach, different textures are represented with various statistical models of the MRF; a Gaussian Markov random field model (Manjunath and Chellappa, 1991; Won and Derin, 1992; Nguyen and Cohen, 1993; Panjwani and Healey, 1995), an augmented state-MRF model (Kervrann and Heitz, 1995), a casual Gaussian autoregressive random field model (Bouman and Liu, 1991), and a generalized Ising model (Andrey and Tarroux, 1998). Recently, the techniques using MRFs have been utilized in a wide range of application areas including image classification of multispectral remotely sensed data (Yamazaki and Gingras, 1999; Hazel, 2000; Sarkar *et al.*, 2002), data generated in real time processing environment (Sziranyi *et al.*,

Received 2 June 2005; Accepted 10 September 2005.

† Corresponding Author: S. – H. Lee (shl@mail.kyungwon.ac.kr)

2000), video sequences (Kim *et al.*, 2000), and high resolution sonar imagery (Mignotte *et al.*, 2000). Lee and Crawford (2005) introduced an MRF-based unsupervised segmentation methods using hierarchical clustering with Bayesian similarity measure. In Lee and Crawford's approach, a multiwindow operation using the boundary blocking was employed to alleviate computational intensiveness of hierarchical clustering.

The fuzzy classification is an EM (expected maximization) iterative approach based on mixture probability distribution (Liang *et al.*, 1992). Under the assumption of a double compound stochastic image process, given an initial class map, this approach iteratively computes the fuzzy membership vectors in the E-step and the maximum likelihood estimates of class-related parameters in the M-step, and when satisfying a convergence condition, generates the optimal class map according to the fuzzy membership vectors. In the double compound image model, the MRF is used to quantify the spatial continuity or smoothness probabilistically, that is, to provide a type of prior information on the region-class process for image classification.

The paper is organized as follows. Section 2 contains a description of the image model associated with the MRF. The fuzzy classification algorithm for image classification is described in Section 3. Experimental results with high-resolution panchromatic and multispectral remotely sensed data are reported in Section 4. Finally, conclusions are stated in Section 5.

2. MRF-based Image Model

A double compound stochastic image process is assumed to combine a discrete-valued field for region-class processes and a continuous random field for observed intensity processes. The MRF is incorporated into digital image analysis by viewing pixel types as states of molecules in a lattice-like physical system defined on a Gibbs random field (GRF) (Georgii, 1979). Due to the MRF-GRF equivalence, the assignment of an energy function to the physical system determines its Gibbs measure, which is used to model molecular interactions, and thus this assignment also determines the MRF. Let $\mathbf{I}_n = \{1, 2, \cdots, N\}$ be the set of indices of pixels in the image. If R_i is the index set of neighbors of the ith pixel, $\mathbf{R} = \{R_i \mid i \in \mathbf{I}_n\}$ is a "neighborhood system" for $\mathbf{I}_n$. A "clique" of $\{\mathbf{I}_n, \mathbf{R}\}$, c is a subset of $\mathbf{I}_n$ such that every pair of distinct indices in c represents pixels which are mutual neighbors, and $\mathbf{C}$ denotes the set of all cliques. A GRF relative to the graph $\{\mathbf{I}_n, \mathbf{R}\}$ on ω is defined as

$$P(\omega) = z^{-1}\exp\{-E(\omega)\}$$
$$E(\omega) = \sum_{c \in C} V_c(\omega) \text{ (energy function)} \qquad (1)$$

where z is a normalizing constant and V_c is a potential function which has the property that it depends only on ω and c. Specification of $\mathbf{C}$ and V_c is sufficient to formulate a Gibbs measure for the region-class model. A particular class of GRF, in which the energy function is expressed in terms of "pair-potentials", is used in this study. The pair-potentials are a family of symmetric functions $\{V_p(i, j) \mid (i, j) \subset \mathbf{I}_n\}$ satisfying $V_p(i, j) = V_p(j, i)$ and $V_p(i, j) = 0$ if $i = j$ or $(i, j) \notin \mathbf{C}_p$ where $\mathbf{C}_p$ is the pair-clique system (see Fig. 1).

It is natural that neighboring pixels with closer intensity levels have a higher probability of being the same class. Based on this idea, spatial continuity can be quantified for image processes with the pair-potentials

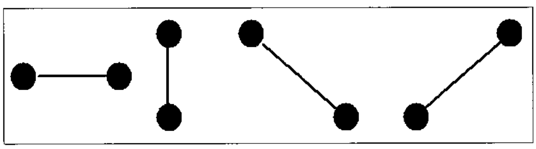

Fig. 1. Pair-clique system for second order.

that are functions of a distance between the neighboring pixels in the mean intensity $\mu(\omega)$, which is a mapping function of ω into real intensity values. The energy function of the MRF is specified in terms of a quadratic function of $\mu(\omega)$ to define the probability structure of the region-class process for the segmentation: if $[\mathbf{v}]^2$ denotes the vector whose elements are squared values of each element of vector $\mathbf{v}$,

$$E_p(\omega) = \sum_{(i,j)\in C_p} \alpha'_{ij}[\mu(\omega_i) - \mu(\omega_j)]^2 \quad (2)$$

where ω_i is the class of the ith pixel, $\mu(\omega_i)$ is the mean intensity vector of class ω_i, and α_{ij} is a non-negative coefficient vector, which represents the "bonding strength" of the ith and the jth pixels.

Without generalization, the observed intensity processes are usually assumed to be Gaussian, and using the MRF associated with the energy function of Eq. (2) for region-class processes, the posterior joint distribution of the class vector ω and the observed intensity process $\mathbf{X}$ is then

$$f(\mathbf{X}, \omega) = f(\mathbf{X} \mid \omega) f(\omega) \propto \exp\{-[\mathbf{X} - \mu(\omega)]'\Sigma^{-1}(\omega)[\mathbf{X} - \mu(\omega)] - E_p(\omega)\} \quad (3)$$

where $\Sigma(\omega)$ is the covariance matrix of the observed intensity process. If Ω is the set of all possible class configurations,

$$\int_\Omega f(\omega)d\omega = 1$$

and the conditional probability is then

$$f(\mathbf{X}|\omega) = \sqrt{2\pi|\Sigma|}^{-1}\exp\{-[\mathbf{X}-\mu(\omega)]'\Sigma^{-1}(\omega)[\mathbf{X}-\mu(\omega)]-E_p(\omega)\}. \quad (4)$$

3. Fuzzy Classication

Consider a problem classifying the image of $\mathbf{I}_n$ in K classes and let the data vector of pixel j, $\mathbf{x}_j$, be associated with an unobserved image class k, which is to be estimated. This association between $\mathbf{x}_j$ and class k can be specified completely with an unobserved indicator vectors, $\mathbf{s}_j = \{s_{kj}, k = 1, \cdots, K\}$. In ideal situation, the kth element of $\mathbf{s}_j$ has unit value and all the other elements are zero if region m belongs to class k. The mixture probability distribution of the complete data set $\mathbf{Z} = \{\mathbf{x}_j, \mathbf{s}_j\}$ is then expressed as

$$F(\mathbf{Z} \mid \mathbf{W}, \Theta) = \prod_{j=1}^{N}\prod_{k=1}^{N} w_k^{s_{kj}} f_k^{s_{kj}}(\mathbf{x}_j \mid \Theta) \quad (5)$$

where $\mathbf{W} = \{w_k\}$ represents the weights of the components $\{f_k\}$ in the mixture distribution, $\Sigma_k w_k = 1$, and $\Theta = \{\mu(\omega), \Sigma(\omega)\}$ is the set of parameters that define the classes. The fuzzy procedure calculates the indicator variables $\{s_{kj}\}$ as fuzzy vectors in the E-step, and the likelihood of $\mathbf{W}$ and Θ is maximized in the M-step using $\{s_{kj}\}$ estimated in the E-step (Ling *et al.*, 1992). For the assumption of additive Gaussian image model, EM iterative approach to compute the fuzzy vector is summarized in Fig. 2.

• **E-step** - Calculating Indicator Vectors.

$$s_{kj}^{(h)} = \frac{w_k^{(h)} f_k(\mathbf{x}_j \mid \Theta^{(h)})}{\sum_k w_k^{(h)} f_k(\mathbf{x}_j \mid \Theta^{(h)})}$$

$$\sum_k s_{kj}^{(h)} = 1$$

$$f_k\left(\mathbf{x}_j \mid \Theta^{(h)}\right) = \sqrt{2\pi\left|\Sigma_k^{(h)}\right|}^{-1} \exp^{-1}\left(\Delta_q + \Delta_p\right)$$

$$\Delta_q = \frac{1}{2}(\mathbf{x}_j - \mu_k^{(h)})'\Sigma_k^{(h)^{-1}}(\mathbf{x}_j - \mu_k^{(h)})$$

$$\Delta_p = \sum_{(j,i)\in C_p} \alpha'_{ji} \sum_{m=1}^{K} s_{mi}^{(h)}[\mu_k^{(h)} - \mu_m^{(h)}]^2$$

• **M-step** - Computing Estimates of $\mathbf{W}$, Θ.

$$w_k^{(h+1)} = \frac{1}{N}\sum_j s_{kj}^{(h)}$$

$$\mu_k^{(h+1)} = \frac{1}{N w_k^{(h+1)}}\sum_j s_{kj}^{(h)}\mathbf{x}_j$$

$$\Sigma_k^{(h+1)} = \frac{1}{N w_k^{(h+1)}}\sum_j s_{kj}^{(h)}(\mathbf{x}_j - \mu_k^{(h+1)})'(\mathbf{x}_j - \mu_k^{(h+1)})$$

Fig. 2. EM iterative approach of fuzzy classification.

4. Experiments

The proposed MRF-based fuzzy classification was first evaluated using simulation data generated by the Monte Carlo method. The methodology was then applied to LANDSAT ETM+ and IKONOS data acquired from two regions on the Korean peninsula respectively.

The 8-bit simulation images of 3 bands were generated using one pattern by adding white Gaussian noise, whose variance is pixel-independent and region-dependent. Thus, the region-class process is characterized by the mean and variance of intensity values. The image pattern of 5 classes, which were used in this section for evaluation of the algorithm, is illustrated in Fig. 3. Fig. 3 also contains the maps of classification errors generated by the fuzzy classifications using different parameters. In the error maps, the misclassified pixels are represented with black. It clearly shows that the MRF-based method is superior to the non-MRF one. In this experiment, the bonding strength coefficients were estimated under the fact that the class variables should be determined such that the corresponding mean intensity fits the observed data in the image classification (Lee and Crawford, 2005), and applied to the classification with being multiplied by different constants. As shown in Fig. 3, the MRF-based scheme yielded a predominant result for an appropriate coefficient, and the classification results were more dependent on the values than the MRF order of the coefficients.

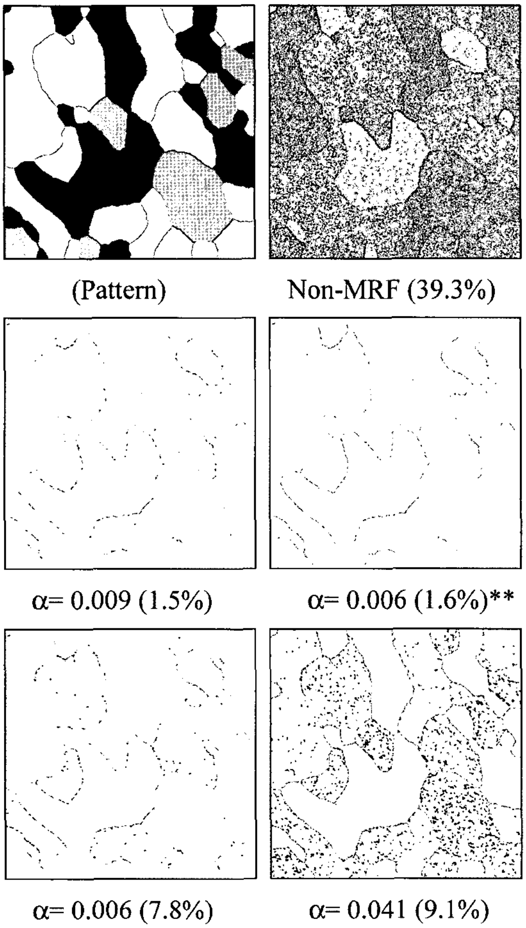

Fig. 3. Pattern of simulation images and error maps of fuzzy classification where misclassified pixels are represented with black dots and error percentages are shown in parenthesis (**: the result using the 2nd order MRF).

The fuzzy classification was applied for LANDSAT ETM+ data observed from Yongin/Nungpyung area in Kyunggi-do, Korea. The image data has 1402×1920 pixels of 3 bands (Green, Red, NIR). Fig. 4 displays the results of 4 classes generated by the fuzzy classification of non-MRF and MRF for a sub-area of Yongin/Nungpyung respectively. The MRF-based

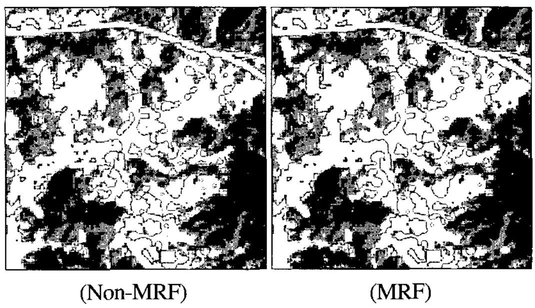

Fig. 4. Classification results of 4 classes using LANDSAT ETM+ data observed from Yongin/Nungpyung area in Kyunggi-do, Korea.

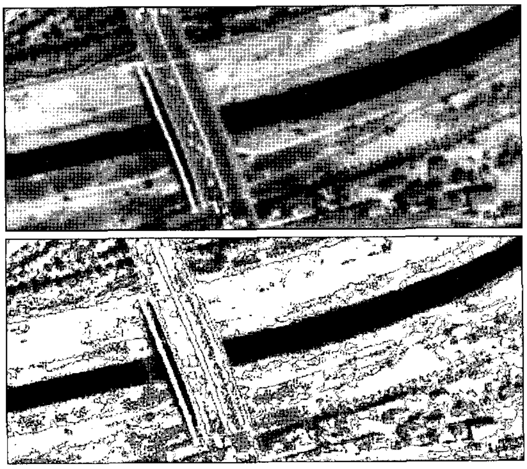

Fig. 5. IKONO panchromatic image observed from Kangnam area in Seoul, Korea and classified map of 4 classes by non-MRF fuzzy classification.

scheme produced more distinctive configuration of the classes than the non-MRF approach. It is more clear in the results generated when applying to a set of IKONOS data acquired over Kangnam area in Seoul, Korea, which has a panchromatic band of 3096 × 3456. Fig. 5 contains the observed image and the result of non-MRF fuzzy approach, and Fig. 6 displays the results generated by the MRF-based EM approach with different number of iterations. For the images of complex ground cover types such as for the data observed from urban area, the small number of iterations may be more appropriate for the EM approach.

5. Conclusions

The experiments with simulation data show that the use of contextual information definitely improves the quality of the classification results for noisy images, and results in reducing the misclassification errors in the inner area of the region, even in the cases where the non-contextual coefficients have better performance in overall accuracy for less noisy images. The MRF-

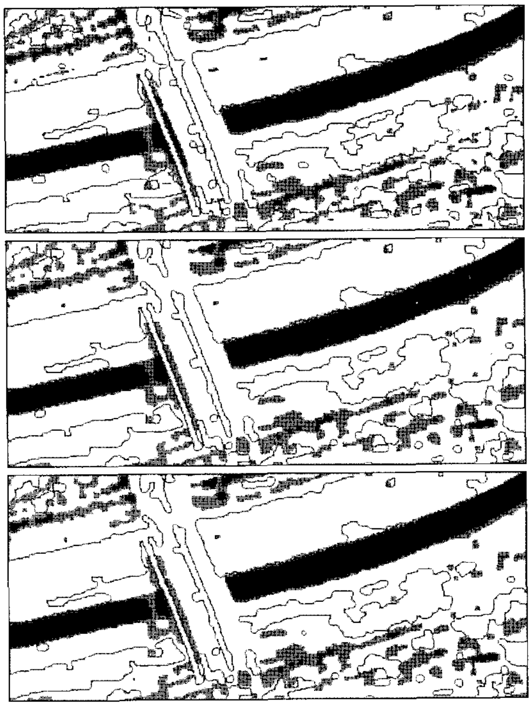

Fig. 6. Classification results of fuzzy classification with 1st-order MRF according to various number of EM iterations (from top, 2 iterations, 10 iterations, 20 iterations).

based approach of the proposed algorithm gains an advantage over the non-MRF classification scheme for the analysis of the patterns with spatial contiguity. The best number of classes can be selected at the level with the maximum ratio of log-likelihood differences in successive numbers of classes (Lee, 2004).

The MRF-based approach can generate an accurate class-map with distinctive class-configuration, especially for spatially continuous imagery. However, the spatial contextual information of MRF may result in wrong classification for the images of complicate (non-smooth) patterns, which comprise target-regions of very small size. Since the classification results vary due to the input parameters used for the algorithm by user, it is difficult to choose the input values for the best classification. Nevertheless, it is not necessary to consider this problem too seriously in practical applications requiring unsupervised analysis. Without knowing the "true" image, there is no globally ideal solution.

Acknowledgements

This study was supported in part by Kyungwon University and the Korean Ministry of Science and Technology. I am appreciative to ETRI and the remote sensing laboratory of Kookmin University for providing the remotely-sensed images used in this study.

References

Andrey, P. and P. Tarroux, 1998. Unsupervised segmentation of Markov random field modeled textured images using selectionist relaxation, *IEEE Trans. Pattern Anal. Machine Intell.*, 20: 252-262.

Bouman, C. and B. Liu, 1991. Multiple resolution segmentation of textured images, *IEEE Trans. Pattern Anal. Machine Intell.*, 13: 99-113.

Hazel, G. G., 2000. Multivariate Gaussian MRF for multispectral scene segmentation and anomaly detection, *IEEE Trans.Geosci. Remote Sensing*, 38: 1199-1211.

Georgii, H. O., 1979. *Canonical Gibbs Measure*, Springer-Verlag, Berlin.

Kervrann, C. and F. Heitz, 1995. A Markov random field model-based approach to unsupervised texture segmentation using local and global spatial statistics, *IEEE Trans. Image Processing*, 4: 856-862.

Kindermann, R. and J. L. Snell, 1982. *Markov Random Fields and Their Application*, Amer. Math. Soc., Providence, R. I..

Lee, S., 2004. Fuzzy training based on segmentation using spatial region growing, *Korean J. Remote Sensing*, 20: 353-359.

Lee S. and M. M. Crawford, 2005. Unsupervised multistage image classification using hierarchical clustering with a bayesian similarity measure, *IEEE Trans. Image Processing*, 14: 312- 320.

Liang, Z, R. J. Jaszczak, and R. E. Coleman, 1992. Parameter Estimation of Finite Mixture Using the EM Algorithm and Information Criteria with Application to Medical Image Processing, *IEEE Trans. Nucl. Sci.*, 39: 1126-1133.

Manjunath, B. S. and R. Chellappa, 1991. Unsupervised texture segmentation using Markov random fields, *IEEE Trans. Pattern Anal. Machine Intell.*, 13: 478-482.

Mignotte, M., C. Coller, P. Perez, and P. Bouthemy, 2000. Sonar image segmentation using an unsupervised hierarchical MRF model, *IEEE Trans. Image Processing*, 9: 1216-1231.

Nguyen, H. H. and P. Cohen, 1993. Gibbs random fields, fuzzy clustering, and the unsupervised segmentation of textured images, *CVGIP: Graphical Models Image Processing*, 55: 1-9.

Panjwani, D. K. and G. Healey, 1995. Markov random field models for unsupervised segmentation of textured color images, *IEEE Trans. Pattern Anal. Machine Intell.*, 17: 939-954.

Sarkar, A., M. K. Biswas, and K. M. S. Sharma, 2000. A simple unsupervised MRF model based image segmentaion approach, *IEEE Trans. Image Processing*, 9: 801-812.

Sarkar, A., M. K. Biswas, B. Kartikeyan, V. Kumar, K. L. Majumder, and D. K. Pal, 2002. A MRF model-based segmentation approach to classification for multispectral imagery, *IEEE*

Trans.Geosci. Remote Sensing, 40:1102-1113.

Sziranyi, T., J. Zerubia, L. Czuni, D. Geldreich, and Z. Kato, 2000. Image segmentation using Markov random field model in fully parallel cellular network architectures, *Real-Time Imaging*, 6: 195-211.

Won, C. S. and H. Derin, 1992. Unsupervised segmentation of noisy and textured images using Markov random fields, *Comp. Vision, Graphics, Image Processing*, 54: 308-328.

Yamazaki, T. and D. Gingras, 1999. Unsupervised multispectral image classification using MRF models and VQ method, *IEEE Trans.Geosci. Remote Sensing*, 37: 1173-1176.